Nuclear Engineering and Technology 54 (2022) 701–708

Contents lists available at ScienceDirect

Nuclear Engineering and Technology

journal homepage: www.elsevier.com/locate/net

Original article

Investigation of gamma radiation shielding properties of polyethylene glycol in the energy range from 8.67 to 23.19 keV

H. Akhdar*, M.W. Marashdeh, M. AlAqeel

Department of Physics, College of Sciences, Imam Mohammad Ibn Saud Islamic University (IMSIU), P.O. Box 90950, Riyadh, 11623, Saudi Arabia

ARTICLE INFO

Article history:
Received 25 May 2021
Received in revised form
20 August 2021
Accepted 23 August 2021
Available online 27 August 2021

Keywords:
Polyethylene glycol (PEG)
Low energy
Geant4
Mass attenuation coefficient
Half value layer
Effective atomic numbers

ABSTRACT

The mass attenuation coefficients (μ_m) of polyethylene glycol (PEG) of different molecular weights (1000 −200,000) were measured using single-beam photon transmission. The X-ray fluorescent (XRF) photons from Zinc (Zn), Zirconium (Zr), Molybdenum (Mo), Silver (Ag) and Cadmium (Cd) targets were used to determine the attenuation of gamma radiation of energy range between 8.67 and 23.19 keV in PEG samples. The results were compared to theoretical values using XCOM and Monte Carlo simulation using Geant4 toolkit which was developed to validate the experiment at those certain energies. The mass attenuation coefficients were then used to compute the effective atomic numbers, electron density and half value layers for the studied samples. The outcomes showed good agreement between experimental and simulated results with those calculated theoretically by XCOM within 5% deviation. The PEG 1000 sample showed slightly higher μ_m value compared with the other samples. The dependence of the photon energy and PEG composition on the values of μ_m and HVL were investigated and discussed. In addition, the values of Z_{eff} and N_{eff} for all PEG samples behaved similarly in the given photon energy range, and they decreased as the photon energy increased.

1. Introduction

Polymers have many applications in various fields due to their different properties as they are easily formed into any desired shape, easy to handle, affordable, and with minimal maintenance. Given the many applications in various fields of polymers, several researchers have investigated the gamma shielding properties of different types of polymers [1–4].

PEGs are polymers synthesized from ethylene oxide, composed repetitions of −O−CH2−CH2 − units and could be synthesized in a wide range of molecular weights which are commercially available and all known to be odorless, colorless, non-toxic, non-immunogenic, amphiphatic and biocompatible [5,6]. PEGs play a very important role in biomedicine as they are used in bioconjugation, drug delivery, surface functionalization and tissue engineering [7–10]. They are also very effective in manufacturing of medical instruments and implants technology as well as biochips and biosensors [11,12].

Research studies focus on PEGs physical properties as they could be used in radiation dosimetry and protection, phantom related technologies as well as medical and nuclear applications. For this reason, researchers are investigating PEGs radiological parameters such as attenuation coefficients, half value layers, effective atomic numbers and interaction cross sections which are essential for choosing and designing shielding material [5,6]. So far, PEG related research is mainly focused on its interaction with radiation of high energy levels [5–13]. Therefore, the gamma attenuation performance of PEG has not been fully studied yet, especially at low energies as it is not tabulated in the literature yet.

Shielding properties of five different samples of PEG were evaluated in this study, when irradiated with gamma radiation at energies ranging from 8.15 to 23.19 keV. First, the data was collected experimentally then compared to those calculated theoretically using XCOM and finally validated with simulation results using Geant4 toolkit. The dependency of the studied parameters on the gamma energy was investigated with the relative differences. The importance of this study comes from the fact that no similar studies has been published yet and that PEG is a very interesting material that could play an important role in many fields such as tomography, X ray and gamma ray fluorescence and radiation biophysics.

* Corresponding author.
E-mail address: hfAkdar@imamu.edu.sa (H. Akhdar).

https://doi.org/10.1016/j.net.2021.08.028

2. Material and method

2.1. Samples preparation

Five different samples with different molecular weights of PEG were studied in this research. The samples were obtained from Sigma-Aldrich (Germany). Each PEG sample was compressed into a thin disk for 5 s using a manual hydraulic press machine. The disk samples have diameters of 1.34 cm and thicknesses of the samples ranged between 0.25 and 0.40 cm with an area of 1.41 cm^2. The basic PEG samples were in the form of chips and melted quickly in the form of thin disks under the press machine, therefore the PEG samples were expressed in term of mass area ranging from 0.32 to 0.47 g/cm^2. Table 1 shows the conventional name and molecular formula of each PEG sample.

2.2. Theory

The main parameter investigated is the mass attenuation coefficient μ_m which could be calculated using Equation (1) [14]:

$$I = I_0 e^{-\mu_m x} \tag{1}$$

Where (I_0) is the monenergetic incident intensity of photons and (I) is the attenuated photons intensity after passing through a mass per unit area (x) layer of a certain material. In case of mixtures and compounds; Equation (2) could be used [14]:

$$\mu_m = \sum_i w_i (\mu_m)_i \tag{2}$$

Where (w_i) is the weight of the ith element.

XCOM is a database that also allows obtaining the photon cross section data for single elements as well as compounds and mixtures, which will be used here to estimate and compare the mass attenuation coefficients of all studied samples [15].

The value of mass attenuation coefficients can lead to the determination of the total atomic cross-section by Equation (3) [16].

$$\sigma_{t,a} = \frac{(\mu_m)_{alloy}}{N_A \sum_i^n (w_i/A_i)} \tag{3}$$

Where (N_A) is Avogradro's number, (A_i) is atomic weight of constituent element of alloy, while the total electronic cross-section for the element is given by Equation (4) [16].

$$\sigma_{t,el} = \frac{1}{N_A} \sum_i^n \frac{f_i A_i}{Z_i} (\mu_{mt})_i \tag{4}$$

Where (f_i) is the number of atoms of element (i) relative to the total number of atoms of all elements in alloy, (Z_i) is the atomic number of the ith element in alloy. The effective atomic number and the mass attenuation coefficient are both very important parameters when it comes to selecting material suitable for radiation dosimetry and detection. The effective atomic number (Z_{eff}) of the compound could be found from the ratio between the total atomic cross-section and the total electronic cross-section through Equation (5) [17–19].

$$Z_{eff} = \frac{\sigma_{t,a}}{\sigma_{t,el}} \tag{5}$$

The half value Layer (HVL) is the thickness of a material that reduces the radiation level by a factor of 2, which could be described by Equation (6), the HVL is very important in radiation related investigations since they predict the required thickness of any radiation shield.

$$HVL = \frac{ln2}{\mu} \tag{6}$$

where (μ) (cm^{-1}) is the linear attenuation coefficient of the material, the relation between the mass attenuation coefficient and the linear attenuation coefficient is given by Equation (7) [17,18].

$$\mu = \mu_m \rho \tag{7}$$

The effective electron density is given by Equation (8) [17,18].

$$N_{eff} = \frac{\mu_m}{\sigma_{t,el}} \tag{8}$$

All these parameters were studied experimentally and theoretically for all five PEG samples of interest.

2.3. Experimental setup

The linear and mass attenuation coefficients were evaluated using single transmitted beam of the X-ray fluorescent (XRF) technique. The annular source of ^{241}Am radioactive source with a 3.7 GBq activity was used to irradiate a pure metal plate to produce XRF energies. The pure metal plates used were Zinc (Zn), Zirconium (Zr), Molybdenum (Mo), Silver (Ag) and Cadmium (Cd) to produce $K_{\alpha 1}$ XRF with photon energies of 8.67, 15.82, 17.51, 22.19 and 23.19 keV, respectively. The experimental setup is shown in Fig. 1. The intensities of the XRF energies were measured using a Si-PIN photodiode XR-100 CR detector (Amptek) with a 1 mil Be window and with an active area and thickness of 7 mm^2 and 300 μm, respectively. The Maestro-ORTEC was used to analyze the detected gamma spectra. Each sample was irradiated for 3600 s to ensure reliable statistic results. A 0.3 cm diameter Lead collimator was used to avoid the detection of any scattered and background radiation. The distances between the pure metal plate and the sample and between the sample and the detector were 17.6 cm and 12.7 cm, respectively. In order to calculate the desired parameters each measurement was repeated three times and the average was obtained, Fig. 1 illustrates the experimental setup used in this study.

2.4. Monte Carlo simulation

Monte Carlo simulations were preformed to validate the parameters of interest using Geant4. Geant4 is a toolkit based on the Monte Carlo statistical method that simulates the passage of particles in matter [19]. The recently released version 10.07 of Geant4 was used to develop a code that simulates the experimental setup in order to study the attenuation coefficients of the five different samples of PEG at different energies to be compared with the experimental results.

A gamma source placed in front a sample of PEG emitting gamma particles in the direction of the sample followed by a 3 mm

Table 1
A list of the conventional name and molecular formula for the PEG samples used in the current study.

Conventional name	Molecular formula
PEG 1000	$C_{44}H_{90}O_{23}$
PEG 10000	$C_{454}H_{910}O_{228}$
PEG 20000	$C_{908}H_{1818}O_{455}$
PEG 100000	$C_{4540}H_{9082}O_{2271}$
PEG 200000	$C_{9080}H_{18162}O_{4541}$

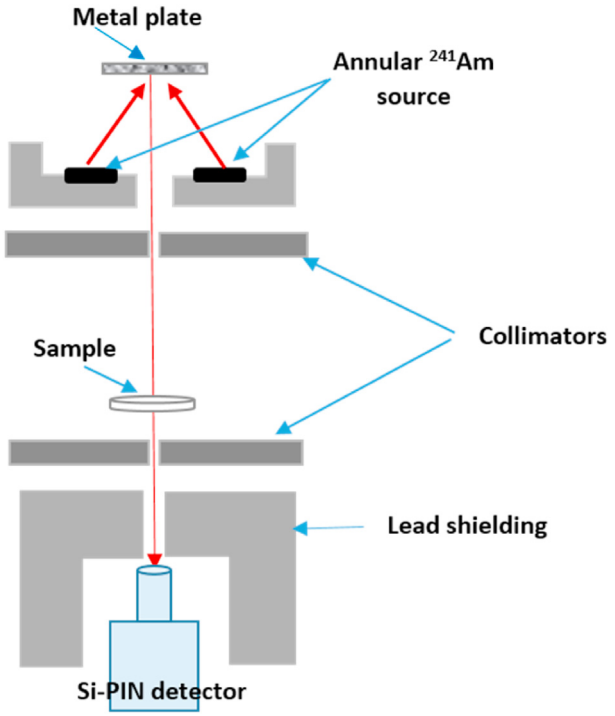

Fig. 1. The experimental setup for measuring XRF attenuation of PEG samples.

pinhole collimator which was placed in front of a detector surrounded by a lead container in order to simulate a narrow beam of mono-energetic gamma rays. Fig. 2 shows a visualization of the simulation code.

In Geant4; the attenuation coefficient can be computed by finding the ratio between the number of gamma particles that reach the detector with and without the sample, then finding the linear attenuation coefficient based on the sample's thickness. The studied energies in this work are low, which means that the interactions of interest are either Compton scattering or photoelectric effect interactions. The attenuation coefficients were found for all five samples of PEG at five different energies.

3. Results and discussion

3.1. Mass attenuation coefficient

The linear and mass attenuation coefficients of the PEG samples were obtained experimentally in the gamma energy range from 8.67 to 23.19 keV as shown in Table 2 using XRF energies within given deviations between 0.0032% and 0.049%. As it was observed that the deviation is slightly higher at photon energy 0f 8.67 keV compared to other photon energies. Table 2 summarizes the experimental results and Fig. 3 represents a comparison between the mass coefficients of all the investigated samples.

The results obtained experimentally were compared to those found using the simulation methods as well as with those found theoretically using XCOM. The mass attenuation coefficients of the studied samples were summarized in Table 3 and they were used to compute other parameters. Root 6.10/04 software was used to plot the mass attenuation coefficients for each sample at different energies as shown in Fig. 3.

It was observed that μ_m coefficient decreases rapidly with the increase of the photon energy, as it was clearly observed in the energy range from 8.67 keV to 23.19 keV. The photoelectric absorption was the main interaction between gamma rays and the PEG samples, therefore, it highly depends on the photon energy and the chemical composition of the PEG samples. In addition, Table 3 shows that the experimentally measured μ_m values were relatively less than the computed values using XCOM. Where this was more evident at the low photon energy of 8.67 keV, as the deviations between the experimental and calculated values for all samples were within the range of 3.48%–4.66%. However, most of the μ_m values evaluated experimentally agree well with μ_m values computed with XCOM with a deviation of less than 3.80% in the photon energies of 15.82, 17.51, 22.19 and 23.19 keV. This can be attributed to the possibility of some impurities in the PEG materials, in addition to the error rate of the XRF experimental setup to evaluate the μm. Moreover, most of the μ_m values measured using Geant4 simulation are in good agreement with μ_m values computed by XCOM within deviations of 5%.

In addition, it can be noted that the differences in the μ_m values for all PEG samples appear more at the energy of 8.67 keV as shown in Fig. 3, as the PEG 1000 sample shows somewhat higher μ_m value compared with the other samples using experimental measurements and simulations.

3.2. Half value layer (HVL)

HVL is an important parameter for any radiation shielding design since the HVL refers to the required thickness of an absorber to reduce the radiation level to half of its initial value. The calculated HVL of PEG samples at the photon energy range 8.67 keV–23.19 keV has been shown in Table 4. The results showed that with the increase photon energy, the HVL value increases. Also, the results showed that the HVL values of the PEG samples were close to each other at the same photon energies. The percentage of difference between experimental and Geant4 simulation results with calculated results by XCOM is within a deviation of 5%.

3.3. Effective atomic number (Z_{eff}) and electron density (N_{eff})

The Z_{eff} and N_{eff} for PEG samples used in the study were evaluated using the value of μ_m from the experiment, the Geant4 simulation and the calculated by XCOM. The Z_{eff} and N_{eff} values for PEG in molecular weights of 1000–200,000 are listed in Table 5 and Table 6. The results of values of the PEG samples fall within the range of the atomic number of their constituent elements ($1 < Z_{eff} < 8$), which matches with other found results for low Z-component materials [5]. The Z_{eff} and N_{eff} values for all the PEG samples behave similarly because all PEG polymer samples have roughly the same chemical composition with small differences in their component weight fraction. Also, the Z_{eff} has highest value at low energy region as the photoelectric effect is dominant at this energy region. The deviation between the XCOM result and experimental and simulation results are within 5% for the studied PEG samples at the selected photon energies. In addition, it is interesting that it was noticed that the results of Geant4 and XCOM show that the PEG 1000 sample has a slightly higher Z_{eff} value, and this indicates that the PEG 1000 is the best shielding material within the studied photon energy region. While the experimental results showed that the PEG 200,000 sample is slightly better in terms of Z_{eff} and N_{eff} values compared with other samples. This indicates that more experimental studies are needed to verify the results at these low photon energies. Table 6 shows the results of N_{eff} for the selected PEG samples and has demonstrated the same behavior of Z_{eff} with photon energy.

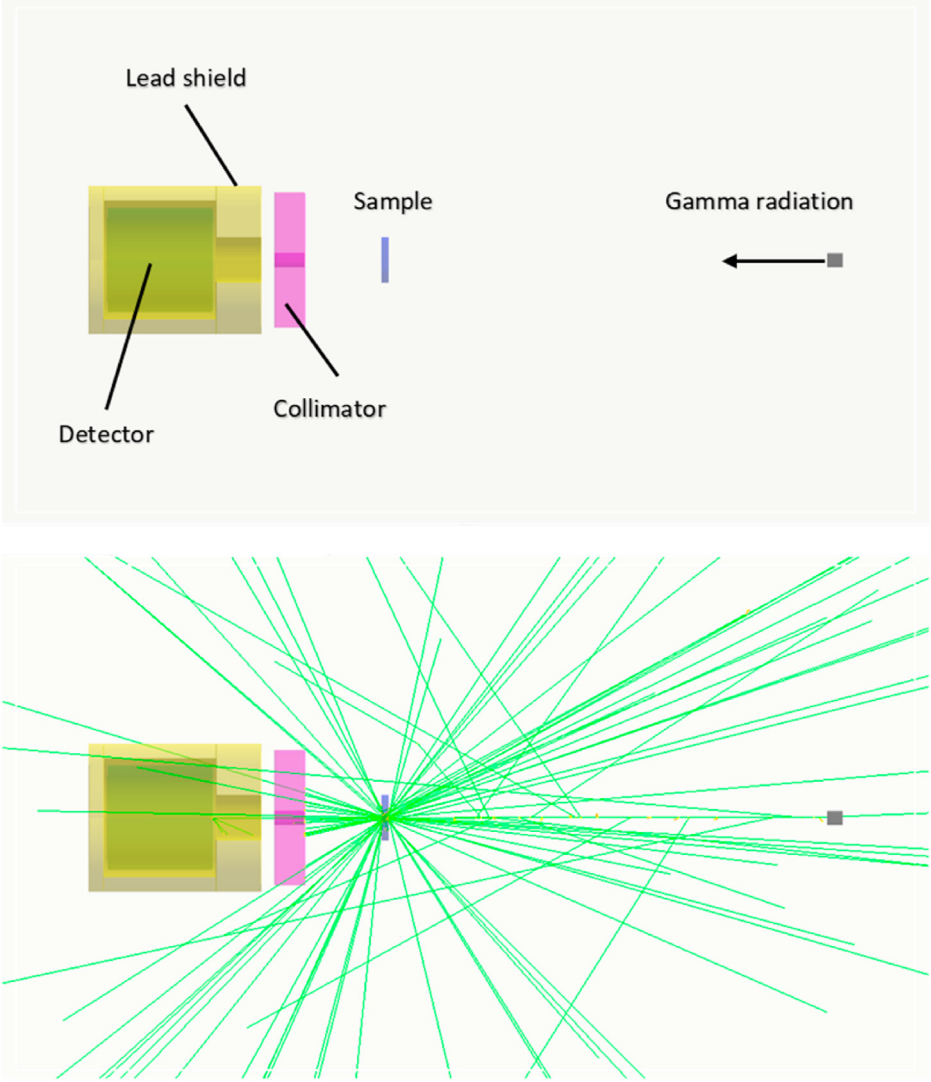

Fig. 2. Visualization of the Geant4 simulation code.

Table 2
Mass attenuation coefficients of the PEG samples measured experimentally.

Energy (keV)	PEG 1000	PEG 10000	PEG 20000	PEG 100000	PEG 200000
Mass attenuation coefficients (cm^2/g)					
8.67	5.147 ± 0.049	5.077 ± 0.043	5.069 ± 0.045	5.099 ± 0.043	5.130 ± 0.038
15.82	0.971 ± 0.0083	0.969 ± 0.0082	0.962 ± 0.0078	0.966 ± 0.0089	0.970 ± 0.0083
17.51	0.768 ± 0.0071	0.767 ± 0.0075	0.764 ± 0.0072	0.768 ± 0.0081	0.769 ± 0.0072
22.19	0.473 ± 0.0069	0.473 ± 0.0049	0.473 ± 0.0057	0.472 ± 0.0066	0.474 ± 0.0047
23.19	0.441 ± 0.0034	0.439 ± 0.0045	0.440 ± 0.0034	0.440 ± 0.0043	0.441 ± 0.0032

4. Conclusion

The shielding properties of selected PEG samples have been investigated. The mass attenuation coefficient (μ_m), HVL, the effective atomic number (Z_{eff}) and the electron density (N_{eff}) have been determined in a gamma energy range from 8.15 to 23.19 keV. The overall results has shown good agreement between the experimental and simulated results with those found theoretically by XCOM within deviations of 5%. This has indicated that at low photon energy range, the photon energy and the composition of the PEG material play an important role in the variation of the μ_m results as the photon interaction is the dominant at these energies. The PEG 1000 sample has shown slightly higher μ_m values compared with the other samples using experimental measurements and simulations. The results has shown that the Z_{eff} and N_{eff} values for all the PEG samples behave similarly at the selected photon energy range and that HVLs for all the PEG samples increase as the photon energy increases. Whereas, the results of the μ_m for PEG samples in molecular weights of 1000–200,000 are not tabulated in the literature therefore, the results can be useful in medicine, nuclear physics and radiological applications in the fields that use low energies in their experimental applications.

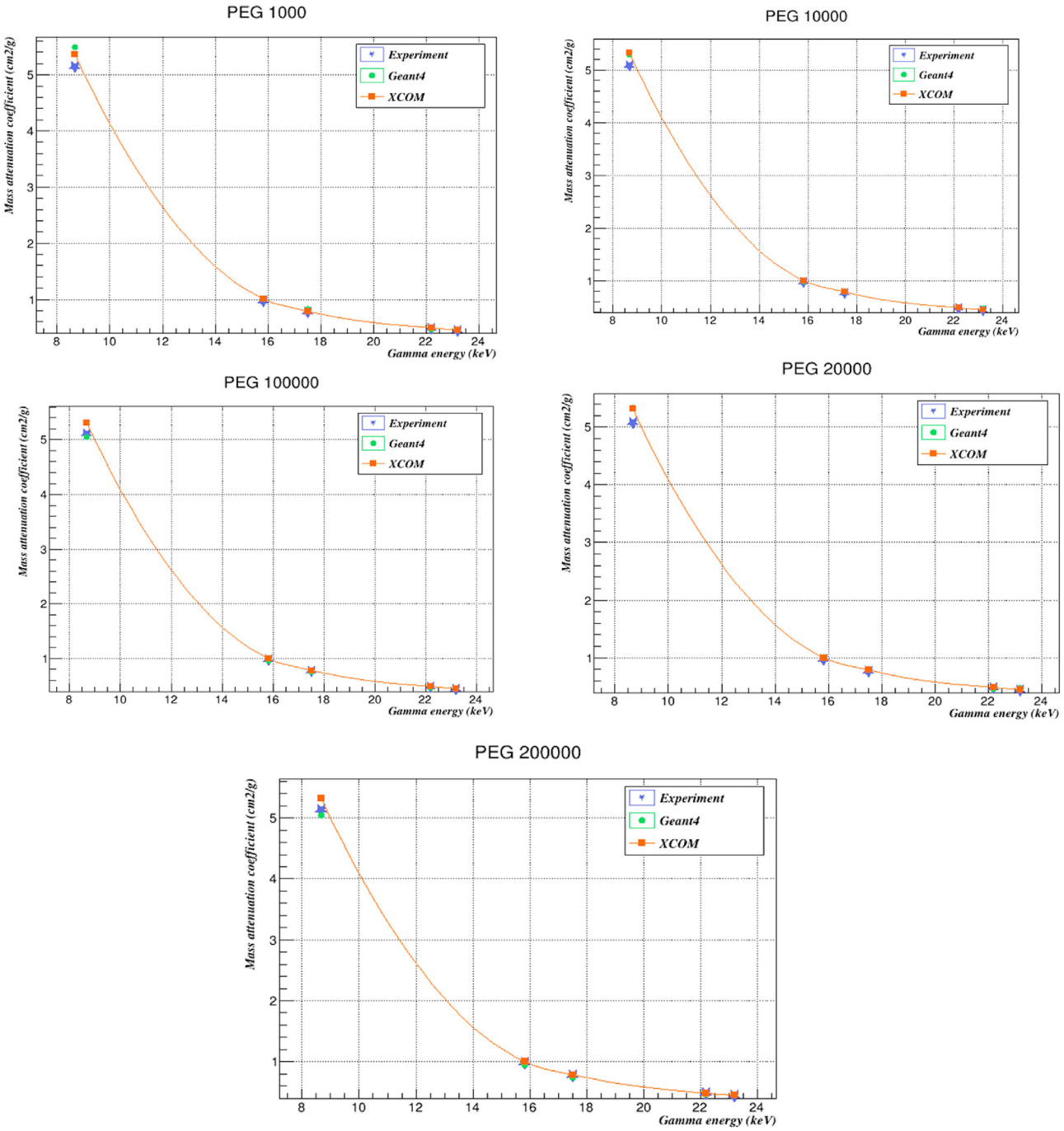

Fig. 3. Mass attenuation coefficients comparison for all five PEG samples found experimentally, estimated theoretically using XCOM and simulated using Geant4.

Table 3
Mass attenuation coefficients (cm^2/g) of the PEG samples measured experimentally, estimated theoretically using XCOM and simulated by Geant4.

Energy (keV)	μ_m (cm^2/g)				
	XCOM	Experiment	Geant4	Percentage deviation (XCOM/Exp.)	Percentage deviation (XCOM/Geant4)
PEG 1000					
8.67	5.367	5.147	5.486	4.10%	−2.22%
15.82	1.007	0.971	1.007	3.57%	0.00%
17.51	0.791	0.768	0.820	2.91%	−3.67%
22.19	0.486	0.473	0.465	2.67%	4.32%
23.19	0.449	0.441	0.468	1.78%	−4.23%
PEG 10000					
8.67	5.320	5.077	5.285	4.57%	0.66%
15.82	1.000	0.969	0.986	3.10%	1.40%
17.51	0.786	0.767	0.808	2.42%	−2.80%
22.19	0.483	0.473	0.482	2.07%	0.21%
23.19	0.447	0.439	0.468	1.79%	−4.70%
PEG 20000					
8.67	5.317	5.069	5.326	4.66%	−0.17%
15.82	1.000	0.962	1.004	3.80%	−0.40%
17.51	0.785	0.764	0.800	2.68%	−1.91%
22.19	0.483	0.473	0.460	2.07%	4.76%
23.19	0.447	0.440	0.469	1.57%	−4.92%
PEG 100000					
8.67	5.315	5.099	5.045	4.06%	5.08%
15.82	0.999	0.966	0.957	3.30%	4.20%
17.51	0.785	0.768	0.749	2.17%	4.59%
22.19	0.483	0.472	0.464	2.28%	3.93%
23.19	0.447	0.440	0.451	1.57%	−0.89%
PEG 200000					
8.67	5.315	5.13	5.045	3.48%	5.08%
15.82	0.999	0.970	0.953	2.90%	4.60%
17.51	0.785	0.769	0.745	2.04%	5.10%
22.19	0.483	0.474	0.462	1.86%	4.35%
23.19	0.447	0.441	0.445	1.34%	0.45%

Table 4
Half value layer (cm) of the PEG samples measured experimentally and simulated by Geant4 compared to XCOM theoretical values.

Energy (keV)	HVL (cm)				
	XCOM	Experiment	Geant4	Percentage deviation (XCOM/Exp.)	Percentage deviation (XCOM/Geant4)
PEG 1000					
8.67	0.108	0.112	0.105	−3.70%	2.86%
15.82	0.574	0.595	0.574	−3.66%	0.00%
17.51	0.730	0.752	0.705	−3.01%	3.55%
22.19	1.190	1.221	1.241	−2.61%	−4.11%
23.19	1.286	1.310	1.234	−1.87%	4.21%
PEG 10000					
8.67	0.109	0.114	0.109	−4.59%	0.00%
15.82	0.578	0.596	0.586	−3.11%	−1.37%
17.51	0.735	0.753	0.715	−2.45%	2.80%
22.19	1.196	1.221	1.198	−2.09%	−0.17%
23.19	1.292	1.316	1.234	−1.86%	4.70%
PEG 20000					
8.67	0.109	0.114	0.108	−4.59%	0.93%
15.82	0.578	0.600	0.575	−3.81%	0.52%
17.51	0.735	0.756	0.722	−2.86%	1.80%
22.19	1.196	1.221	1.255	−2.09%	−4.70%
23.19	1.293	1.313	1.231	−1.55%	5.04%
PEG 100000					
8.67	0.109	0.113	0.114	−3.67%	−4.39%
15.82	0.578	0.598	0.604	−3.46%	−4.30%
17.51	0.736	0.752	0.771	−2.17%	−4.54%
22.19	1.197	1.224	1.246	−2.26%	−3.93%
23.19	1.293	1.313	1.281	−1.55%	0.94%
PEG 200000					
8.67	0.109	0.113	0.114	−3.67%	−4.39%
15.82	0.578	0.596	0.606	−3.11%	−4.62%
17.51	0.736	0.751	0.775	−2.04%	−5.03%
22.19	1.197	1.219	1.250	−1.84%	−4.24%
23.19	1.293	1.310	1.299	−1.31%	−0.46%

Table 5
The effective atomic number of the studied samples.

Energy (keV)	Z_{eff}				
	XCOM	Experiment	Geant4	Percentage deviation (XCOM/Exp.)	Percentage deviation (XCOM/Geant4)
PEG 1000					
8.67	6.861	6.578	7.011	−4.125%	−2.186%
15.82	5.858	5.645	5.854	3.636%	0.068%
17.51	5.589	5.422	5.789	2.988%	−3.578%
22.19	4.935	4.804	4.723	2.655%	4.296%
23.19	4.819	4.726	5.016	1.930%	−4.088%
PEG 10000					
8.67	6.842	6.527	6.794	4.604%	0.702%
15.82	5.841	5.658	5.758	3.133%	1.421%
17.51	5.573	5.437	5.728	2.440%	−2.781%
22.19	4.923	4.818	4.910	2.133%	0.264%
23.19	4.808	4.719	5.030	1.851%	−4.617%
PEG 20000					
8.67	6.841	6.519	6.849	4.707%	−0.117%
15.82	5.841	5.619	5.864	3.801%	−0.394%
17.51	5.573	5.417	5.673	2.799%	−1.794%
22.19	4.923	4.819	4.687	2.113%	4.794%
23.19	4.807	4.730	5.042	1.602%	−4.889%
PEG 100000					
8.67	6.840	6.559	6.490	4.108%	5.117%
15.82	5.840	5.643	5.591	3.373%	4.264%
17.51	5.572	5.447	5.312	2.243%	4.666%
22.19	4.922	4.810	4.728	2.275%	3.941%
23.19	4.807	4.731	4.849	1.581%	−0.874%
PEG 200000					
8.67	6.840	6.599	6.490	3.523%	5.117%
15.82	5.840	5.667	5.568	2.962%	4.658%
17.51	5.572	5.454	5.284	2.118%	5.169%
22.19	4.922	4.830	4.708	1.869%	4.348%
23.19	4.807	4.741	4.784	1.373%	0.478%

Table 6
The effective electron density of the studied samples.

Energy (keV)	N_{eff} x 10^{23} (e^-/cm^2)				
	XCOM	Experiment	Geant4	Percentage deviation (XCOM/Exp.)	Percentage deviation (XCOM/Geant4)
PEG 1000					
8.67	6.571	6.301	6.716	4.109%	−2.207%
15.82	5.611	5.407	5.607	3.636%	0.071%
17.51	5.353	5.194	5.546	2.970%	−3.605%
22.19	4.727	4.602	4.524	2.644%	4.294%
23.19	4.616	4.527	4.805	1.928%	−4.094%
PEG 10000					
8.67	6.548	6.247	6.503	4.597%	0.687%
15.82	5.590	5.416	5.511	3.113%	1.413%
17.51	5.334	5.204	5.482	2.437%	−2.775%
22.19	4.712	4.612	4.700	2.122%	0.255%
23.19	4.601	4.516	4.815	1.847%	−4.651%
PEG 20000					
8.67	6.546	6.239	6.555	4.690%	−0.137%
15.82	5.589	5.378	5.613	3.775%	−0.429%
17.51	5.333	5.185	5.429	2.775%	−1.800%
22.19	4.711	4.613	4.486	2.080%	4.776%
23.19	4.601	4.527	4.826	1.608%	−4.890%
PEG 100000					
8.67	6.545	6.277	6.211	4.095%	5.103%
15.82	5.588	5.401	5.351	3.346%	4.241%
17.51	5.332	5.213	5.084	2.232%	4.651%
22.19	4.710	4.603	4.525	2.272%	3.928%
23.19	4.600	4.528	4.641	1.565%	−0.891%
PEG 200000					
8.67	6.545	6.316	6.211	3.499%	5.103%
15.82	5.588	5.424	5.328	2.935%	4.653%
17.51	5.332	5.220	5.057	2.101%	5.158%
22.19	4.710	4.623	4.506	1.847%	4.331%
23.19	4.600	4.538	4.579	1.348%	0.457%

Declaration of competing interest

The authors declare that they have no known competing financial interests or personal relationships that could have appeared to influence the work reported in this paper.

Acknowledgements

The authors are highly thankful to Mr. Yayha Mobarki in Nuclear and Radiological Regulatory Commission for providing the facilities to conduct the experiments.

References

[1] T. Singh, Rajni, U. Kaur, P.S. Singh, Photon energy absorption parameters for some polymers, Ann. Nucl. Energy 37 (2010) 422–427, https://doi.org/10.1016/j.anucene.2009.12.017.
[2] K.S. Mann, A. Rani, M.S. Heer, Shielding behaviors of some polymer and plastic materials for gamma-rays, Radiat. Phys. Chem. 106 (2015) 247–254, https://doi.org/10.1016/j.radphyschem.2014.08.005.
[3] M.S. Al-Buriahi, C. Eke, S. Alomairy, A. Yildirim, H.I. Alsaeedy, C. Sriwunkum, Radiation attenuation properties of some commercial polymers for advanced shielding applications at low energies, Polym. Adv. Technol. 32 (2021) 2386–2396, https://doi.org/10.1002/pat.5267.
[4] M.I. Sayyed, Investigation of shielding parameters for smart polymers, Chin. J. Phys. 54 (2016) 408–415, https://doi.org/10.1016/j.cjph.2016.05.002.
[5] M. Kurudirek, Effective atomic number, energy loss and radiation damage studies in some materials commonly used in nuclear applications for heavy charged particles such as H, C, Mg, Fe, Te, Pb and U, Radiat. Phys. Chem. 122 (2016) 15–23, https://doi.org/10.1016/j.radphyschem.2016.01.012.
[6] S. Haoue, H. Derdar, M. Belbachir, A. Harrane, A new green catalyst for synthesis of bis-macromonomers of polyethylene glycol (PEG), ChChT 14 (2020) 468–473, https://doi.org/10.23939/chcht14.04.468.
[7] I.F. Al-Hamarneh, M.W. Marashdeh, F.I. Almasoud, A. Alkaoud, Determination of gamma-ray parameters for polyethylene glycol of different molecular weights, Nucl. Sci. Tech. 28 (2017), https://doi.org/10.1007/s41365-017-0311-y.
[8] Bioconjugate Techniques, Elsevier, 2008, https://doi.org/10.1016/b978-0-12-370501-3.x0001-x.
[9] W. Mccarthy, Polymeric drug delivery techniques, Aldrich Mater. Sci. (2016) 3–12.
[10] J. Manson, D. Kumar, B.J. Meenan, D. Dixon, Polyethylene glycol functionalized gold nanoparticles: the influence of capping density on stability in various media, Gold Bull. 44 (2011) 99–105, https://doi.org/10.1007/s13404-011-0015-8.
[11] B.D. Fairbanks, M.P. Schwartz, C.N. Bowman, K.S. Anseth, Photoinitiated polymerization of PEG-diacrylate with lithium phenyl-2,4,6-trimethylbenzoylphosphinate: polymerization rate and cytocompatibility, Biomaterials 30 (2009) 6702–6707, https://doi.org/10.1016/j.biomaterials.2009.08.055.
[12] A. Larsson, T. Ekblad, O. Andersson, B. Liedberg, Photografted poly(ethylene glycol) matrix for affinity interaction studies, Biomacromolecules 8 (2007) 287–295, https://doi.org/10.1021/bm060685g.
[13] F. Brétagnol, H. Rauscher, M. Hasiwa, O. Kylián, G. Ceccone, L. Hazell, A.J. Paul, O. Lefranc, F. Rossi, The effect of sterilization processes on the bioadhesive properties and surface chemistry of a plasma-polymerized polyethylene glycol film: XPS characterization and L929 cell proliferation tests, Acta Biomater. 4 (2008) 1745–1751, https://doi.org/10.1016/j.actbio.2008.06.013.
[14] J.H. Hubbell, Photon mass attenuation and energy-absorption coefficients, Int. J. Appl. Radiat. Isot. 33 (1982) 1269–1290, https://doi.org/10.1016/0020-708x(82)90248-4.
[15] L. Gerward, N. Guilbert, K.B. Jensen, H. Levring, WinXCom—a program for calculating X-ray attenuation coefficients, Radiat. Phys. Chem. 71 (2004) 653–654, https://doi.org/10.1016/j.radphyschem.2004.04.040.
[16] K. Singh, H. Singh, V. Sharma, R. Nathuram, A. Khanna, R. Kumar, S. Singh Bhatti, H. Singh Sahota, Gamma-ray attenuation coefficients in bismuth borate glasses, Nucl. Instrum. Methods Phys. Res. Sect. B Beam Interact. Mater. Atoms 194 (2002) 1–6, https://doi.org/10.1016/s0168-583x(02)00498-6.
[17] J. Kaewkhao, J. Laopaiboon, W. Chewpraditkul, Determination of effective atomic numbers and effective electron densities for Cu/Zn alloy, J. Quant. Spectrosc. Radiat. Transf. 109 (2008) 1260–1265, https://doi.org/10.1016/j.jqsrt.2007.10.007.
[18] A. Madhusudhan Rao, K. Narender, K. Gopal Kishan Rao, N. Gopi Krishna, R. Krishna Murthy, Mass attenuation coefficients, effective atomic and electron numbers of alkali halides for multi-energetic photons, Res. J. Phys. Sci. Res. J. Phys. Sci. 1 (2013).
[19] S. Agostinelli, J. Allison, K. Amako, J. Apostolakis, H. Araujo, P. Arce, M. Asai, D. Axen, S. Banerjee, G. Barrand, F. Behner, L. Bellagamba, J. Boudreau, L. Broglia, A. Brunengo, H. Burkhardt, S. Chauvie, J. Chuma, R. Chytracek, G. Cooperman, G. Cosmo, P. Degtyarenko, A. Dell'Acqua, G. Depaola, D. Dietrich, R. Enami, A. Feliciello, C. Ferguson, H. Fesefeldt, G. Folger, F. Foppiano, A. Forti, S. Garelli, S. Giani, R. Giannitrapani, D. Gibin, J.J. Gómez Cadenas, I. González, G. Gracia Abril, G. Greeniaus, W. Greiner, V. Grichine, A. Grossheim, S. Guatelli, P. Gumplinger, R. Hamatsu, K. Hashimoto, H. Hasui, A. Heikkinen, A. Howard, V. Ivanchenko, A. Johnson, F.W. Jones, J. Kallenbach, N. Kanaya, M. Kawabata, Y. Kawabata, M. Kawaguti, S. Kelner, P. Kent, A. Kimura, T. Kodama, R. Kokoulin, M. Kossov, H. Kurashige, E. Lamanna, T. Lampén, V. Lara, V. Lefebure, F. Lei, M. Liendl, W. Lockman, F. Longo, S. Magni, M. Maire, E. Medernach, K. Minamimoto, P. Mora de Freitas, Y. Morita, K. Murakami, M. Nagamatu, R. Nartallo, P. Nieminen, T. Nishimura, K. Ohtsubo, M. Okamura, S. O'Neale, Y. Oohata, K. Paech, J. Perl, A. Pfeiffer, M.G. Pia, F. Ranjard, A. Rybin, S. Sadilov, E. Di Salvo, G. Santin, T. Sasaki, N. Savvas, Y. Sawada, S. Scherer, S. Sei, V. Sirotenko, D. Smith, N. Starkov, H. Stoecker, J. Sulkimo, M. Takahata, S. Tanaka, E. Tcherniaev, E. Safai Tehrani, M. Tropeano, P. Truscott, H. Uno, L. Urban, P. Urban, M. Verderi, A. Walkden, W. Wander, H. Weber, J.P. Wellisch, T. Wenaus, D.C. Williams, D. Wright, T. Yamada, H. Yoshida, D. Zschiesche, Geant4—a simulation toolkit, Nucl. Instrum. Methods Phys. Res. Sect. A Accel. Spectrom. Detect. Assoc. Equip. 506 (2003) 250–303, https://doi.org/10.1016/s0168-9002(03)01368-8.